Reconstructing Historical Urban Landscapes from KH-9 HEXAGON Mapping Camera System Imagery: An Example of Hangzhou City

Amir Reza Shahtahmassebi[1], Danni Huang[1], Jie Lu[1], Erling Li[2], Xiaoli Huang[1], Ling Jiang[1], Golnaz Shahtahmassebi[3], Nathan Moore[4]， Peter M. Atkinson[5],

[1]*School of Geographic Information and Tourism, Chuzhou University, Chuzhou， China*

[2]*Institute of Sustainable Development in Agriculture and Rural Area, Henan University, Kaifeng, Henan, China*

[3]*Department of Physics and Mathematics, School of Science and Technology, Nottingham Trent University, Nottingham, UK*

[4]*Department of Geography, Michigan State University, East Lansing, MI 48823, USA*

[5]*Faculty of Science and Technology, Lancaster University, Bailrigg, Lancaster LA1 4YQ, UK*

*Corresponding authors: amirreza208@hotmail.com;

Reconstructing Historical Urban Landscapes from KH-9 HEXAGON Mapping Camera System Imagery: An Example of Hangzhou City

Declassified images from the Keyhole (KH)-9 HEXAGON mapping camera system (MCS) offer fine-scale details of urban regions. However, these images have seldom been utilized in urban research due to challenges in labelling (collecting training samples), having only a single panchromatic band and classification. To tackle these limitations, this paper focuses on developing a multi-stage reconstructed historical fine-scale urban landscape (RHFUL) pipeline for KH-9 HEXAGON MCS. The proposed pipeline first integrates internalized parameters, hierarchical object-based image analysis properties and class variability to synthesize new features, abbreviated to IHC. Second, the pipeline uses a weak semi-automated supervised labelling (WSSL) approach to acquire training samples. Finally, the training samples and generated features are subjected to the SegNet deep learning architecture. The performance of each step was assessed against corresponding state-of-the-art benchmark approaches for each of synthesizing features, labelling and classification. In the proposed RHFUL pipeline, the proposed IHC provided the most salient information for urban classification, WSSL labelled urban features more accurately, and the SegNet architecture classified more accurately the urban features relative to the benchmarks. Considering the potential advantages, but also limitations of KH-9 HEXAGON MCS images, further research should be undertaken, particularly drawing on the current advances in pattern recognition techniques for contemporary digital satellite sensors.

Keywords: KH-9 HEXAGON, mapping camera system (MCS), historical urban landscape, labelling, synthesizing features, deep learning.

1. Introduction

Fine spatial resolution (FSR) satellite sensor imagery has opened new opportunities for extracting fine-scale spatial details on urban landscapes (Lv *et al.*, 2023a; Lv *et al.*, 2023b; Lv *et al.*, 2023c). However, because FSR satellite sensors were launched after 2000, there is a scarcity of FSR data before 2000 (Marzolff *et al.*, 2022). Declassified photographs from the archives of KH-9 HEXAGON, one of the satellite missions of the U.S. Keyhole (KH) program, are able to narrow this information gap (Dehecq *et al.*, 2020). KH-9 HEXAGON (hereafter KH-9) captured photographs of nearly all the Earth's surface (excluding Greenland, Antarctica and Australia) from 1972 to 1986 (Hammer *et al.*, 2022). KH-9 included two cameras: the mapping camera system (MCS) and the panoramic camera system (PCS) (Hammer *et al.*, 2022). This research focuses on MCS imagery. The MCS imagery has a spatial resolution of 6 to 9 m with a single panchromatic band (Fowler, 2016). The KH-9 MCS has the advantage of having been in operation four to five decades ago when no FSR satellite imagery was available (see supplementary: Figure 1). Photographs from the KH-9 archive were declassified in 2002 (Fowler, 2016), and converted from analogue photographs into digital imagery which can be downloaded via EarthExplorer (http://earthexplorer.usgs.gov).

Although KH-9 MCS images were used in various disciplines, these images have been greatly under-utilized in urban research (Shahtahmassebi *et al.*, 2023). Arguably, there are three bottlenecks: single panchromatic band limitations, labelling and classification. Given the complexities of urban landscapes, the single panchromatic band is generally insufficient for urban mapping purposes and reconstructing historical fine-scale urban landscapes (RHFUL) (Pacifici *et al.*, 2009) (see supplementary: Figure 2). Moreover, collecting urban labels (training samples) based on this imagery or other historical remote sensing imagery is a non-trivial task (Mboga *et al.*, 2020). Finally, the complexity and diversity of historical urban patterns in analogue panchromatic KH-9 MCS imagery makes RHFUL a challenging task. This is because most newer classification techniques such as deep learning were developed for imagery acquired by digital sensors (see supplementary: Figure 3). Given the limitations associated with the outdated film-based panchromatic KH-9 MCS imagery technology and the aforementioned issues, three main research questions arise:

(1) Using KH-9 MCS, how can we effectively employ feature synthesis approaches to leverage urban spatial-contextual information for classification?
(2) What type of labelling techniques are appropriate for KH-9 MCS over urban regions?
(3) Which classification systems are the most efficient for reconstructing historical urban landscapes from KH-9 MCS images?

The overarching aim of this research was, thus, to develop a multi-stage pipeline for RHFUL using KH-9 MCS imagery. The specific contributions of this research are: (1) An approach for synthesizing features is devised to both compensate for the lack of multispectral bands, and maintain and improve the salient properties of image objects at fine-resolution from KH-9 MCS, (2) A semi-automatic supervised labelling framework is developed for collecting historical labels for the classification system, and (3) A deep learning architecture is proposed to reconstruct historical urban regions from the KH-9 MCS imagery. We also compare this pipeline of approaches to several state-of-the-art techniques for synthesizing features, labelling and image classification.

2. Study area and data

The study area was set in Hangzhou city, capital of Zhejiang Province in China. This study area was chosen to encompass a highly diverse range of urban landscape categories. Specifically, a 100 km^2 study area covering most of the urban landscape was selected comprising impervious surfaces, natural covers (e.g., water bodies, urban forests and farmlands) and semi-natural covers (e.g., recreational regions).

The KH-9 MCS panchromatic image covering the study area was downloaded via EarthExplorer (http://earthexplorer.usgs.gov). This image was acquired on 18 December, 1975 (mission 1211-5, frame 7: DZB1211-500049L007001_a), with a geometric resolution of approximately 6-9 m. The study area was manually digitized and masked out from the KH-9 MCS image. The extracted image was then subjected to a wavelet transform and multi-resolution Top_hat filter for de-noising and contrast enhancement, respectively. A detailed description of these approaches is given in Shahtahmassebi *et al.* (2023).

Besides the KH-9 MCS imagery, ancillary data including a Hangzhou City Map from 1983, historical photographs of Hangzhou City, and Google Earth archives were also collected for analytical purposes.

3. Methodology

The RHFUL pipeline consisted of three steps: synthesizing features, labelling, and classification. Each step was evaluated against corresponding benchmarks. These are each described in detail in this section.

3.1. Proposed synthesizing features approach and benchmarks

To compensate for the lack of multispectral bands in the KH-9 MCS image, we devised an approach to synthesize new features. The proposed approach integrates internalized parameters, hierarchical object-based image analysis properties and class variability. As such, this approach is abbreviated to IHC. This approach considers preserving the salient properties of image objects, thus, enhancing the available information on historical urban conditions at a fine-resolution. The details of these variables are as follows:

(1) Internalized parameters:

Internalized parameters include a combination of per-pixel, object and morphological features. The internalization is computed as:

$$\mathrm{Intern}_{\mathrm{scale}} = \frac{\mathrm{HOBIA}_{\mathrm{Scale}} + \mathrm{MPPL}_{\mathrm{Scale}} + \mathrm{MMO}_{\mathrm{Scale}}}{n} \quad (1)$$

where 'Intern' is internalization, 'HOBIA' is hierarchical object-based image analysis, 'MPPL' is multiple-scale per-pixel layers and 'MMO' is multi-scale morphological operators. "Scale" represents the window size in MPPL and MMO, and segmentation level in HOBIA. '*n*' is the number of images, herein set as 3.

MPPL characterizes the relationship between a pixel and its specific neighbours. MPPL was computed using the Gray Level Co-occurrence Matrix (GLCM)-mean texture with window sizes: 3×3 and 7×7 pixels.

The MMO captures the spatial characteristics of image features. MMOs are calculated using opening-closing by reconstruction based on structure elements (SEs) with a square shape at two scales: 3×3 and 7×7. Opening is defined as the dilation of an eroded image which eliminates brighter areas while closing is considered as the erosion of a dilated image that filters darker regions (Soille, 2003).

In this procedure, opening was applied firstly to the KH-9 MCS image. The obtained result was then subjected to the closing operator to achieve opening-closing by reconstruction. This method better maintains the shape of image objects in comparison to conventional opening-closing filters (Shahtahmassebi *et al.*, 2023).

Image segmentation can be achieved generally in two ways: (1) generating several independent segmented layers and (2) producing hierarchical segmented layers where each layer is established above or below the former level (i.e., HOBIA) (Benz *et al.*, 2004). HOBIA has the advantage of offering spatial hierarchy (e.g., super-object relationships, neighbouring objects) between segmented layers. In this research, we designed seven hierarchical segmented layers using an 'above layer' algorithm. In this algorithm, each segmented layer has a super-level (coarse-scale) above it, where multiple objects (fine-scale) are assigned to a single object. The 'above layer' algorithm was constructed via a multi-resolution segmentation technique. The multi-resolution segmentation parameters are scale, shape/colour and smoothness/compactness (Please see supplement: Table 1). Among the six layers, we selected two layers (levels 3 and 5) which represented sub- and super-objects. eCognition® (eCognition Developer Trimble Germany, 2014) technology was used to establish HOBIA.

(2) HOBIA properties

We extracted HOBIA properties for the above segmented layers. These are: shape features (shape index, roundness, compactness, rectangular fit), topological relationship (mean difference neighbourhood), spatial hierarchy (super object relationship), a positional feature (maximum latitude) and GLCM measures (entropy, correlation, dissimilarity) (Geiss *et al.*, 2016).

(3) Class variability

To capture inter- and intra-class variability, we applied a watershed transform, established through three cascade steps. First, the KH-9 MCS image was subjected to opening-closing operators with a multi-scale (1×1, 3×3) SE in a disk shape. The result was subjected to a Gaussian low pass filter with window size 11×11 to minimize the impact of any noise within the image. The watershed transform was then applied to the filtered image. Finally, the internalized layers (two layers), HOBIA properties and class variability were stacked into a single layer (i.e., IHC).

The performance of the IHC was compared with single panchromatic (SP) and three texture-synthesizing methods: per-pixel Gray Level Co-occurrence Matrix (GLCM) textures, integration of morphological operators and gradients (MOsG), and Gabor texture. The GLCM textures were designed by calculating the mean, dissimilarity, entropy and correlation with window sizes: 3×3, 5×5, 7×7 and 9×9 (Pacifici *et al.*, 2009).

For MOsG, opening-closing (see Step No.2 for definition of opening-closing) was applied to the KH-9 MCS image with structuring elements (SE): 3×3, 5×5, 7×7 and 9×9. Additionally, we calculated external (r^+) and internal (r^-) gradients using the difference between the original image (I), dilation (d) and erosion (e) with respect to the corresponding SE, which are (Soille, 2003):

$$r^- = I - e_{SE} \tag{2}$$

$$r^+ = d_{SE} - I \tag{3}$$

The Gabor textures were generated with wavelengths of 2,4,6,8 and 10 (in pixels/cycle), and orientations between 0 and 120 (in degrees, in steps of 30 degrees). The generated textures were subjected to normalization.

3.2. Proposed labelling approach and benchmarks

To tackle the labelling problem, we utilized a weak semi-automated supervised labelling (WSSL) approach. First, we carefully identified several no-change urban features in Hangzhou City in the KH-9 MCS image with the aid of the 1983 Hangzhou land cover map along with historical archives of Hangzhou photographs and Google Earth archives (see supplementary: Figure 4). The identified urban features were divided into 14 categories: roads, built-up roofs, lakes, ponds, rivers, forested regions, rural areas, parks, urban green spaces, topographic shadow, built-up shadow, farmland, parking lots and residential areas. The IHC layer was then classified initially using a support vector machine (SVM) applied to these urban features. The SVM parameters were: cost parameter (500), kernel (radial basis function) and maximum iteration (5000).

To assess the performance of the proposed WSSL, we used fully-automatic unsupervised Segment Anything Models (SAM) which included three deep learning models: vit_h, vit_l and vit_b (Kirillov *et al.*, 2023). It is noteworthy that the SAM models were pre-trained only for colour composite layers (three bands). Thus, the "cv2" function in python was used to convert the single panchromatic band of KH-9 MCS into a composite layer. This research focused only on the overall accuracy (OA) of the generated label maps.

3.3. Proposed classification strategy and benchmarks

Given the promising performance of deep learning classification for historical aerial photographs (Mboga *et al.*, 2020) and the lack of documented research for KH-9 MCS images, we utilized the SegNet architecture in the RHFUL pipeline. SegNet applies shortcut connections in its architecture and, thus, is more efficient than without these (Badrinarayanan *et al.*, 2017). We used a learning rate of 0.05, a stochastic gradient descent optimization with momentum (0.9), along with weight decay (0.0001), mini-batch size (16) and maximum number of epochs (25). Due to the imbalanced nature of sparse urban land classes, class weighting based on inverse frequency weighting was applied in the pixel layer classification. To feed the SegNet, the KH-9 MCS image and the generated labels map were cropped individually into image patches with a size of

100×100 pixels. In the experimental process, 1518 patches were used for training and 102 patches for validation.

To evaluate the performance of the proposed SegNet, we considered four image benchmark methods (random forest (RF), radial basis function (RBF) neural network, self-organizing map (SOM) and Unet architecture). The generated labels map and predefined parameters were also used for these classifiers. It is noteworthy that urban classes were merged into the seven major categories after classification. These are: 'Bright_impervious surfaces (IS)'- e.g., roads, 'Dark_impervious surface (IS)' - e.g., built-up roofs, 'Non_impervious surfaces (IS)' - e.g., farmlands, 'Water' - e.g., rivers, 'Shadow' - .e.g., topographic shadows, 'Semi_natural' - e.g., recreational, and 'Forest' - e.g., urban forest.

3.4. Accuracy assessment

The accuracy of the generated RHFUL maps was assessed by the overall accuracy (OA), Kappa coefficient (κ) and Jaccard micro index (JDMI) (a measure of similarity). The accuracy of each urban class was gauged by the recall (RC) and precision (PR). 30% of urban classes in the urban labels map were selected randomly for calculating these metrics. The generated RHFUL maps were not subjected to post-classification processing (e.g., noise removal) to ensure the results reflected the real effects of the classification systems.

4. Results

Figure 1(a) shows that the proposed WSSL method effectively and accurately (OA: 95%) characterized the semantic contents of this complex historical urban landscape compared with other benchmark methods (OA: less than 10%). Hence, the proposed WSSL labels map was selected for subsequent procedures.

In terms of feature synthesizing, careful comparison between the proposed IHC approach (Figure 1(b)) and benchmark methods (Figure 1(c)) shows that IHC yielded the smoothest visual results with reliable boundaries. Importantly, some semantic features of the historical urban landscape were effectively identified with reliable geometric fidelity. For example, urban forested regions (Figure 1(b-ii): dark green colour) were distinguished correctly by IHC (Figure.1 (b-i)) in comparison with the benchmark methods and a single panchromatic (SP) band (Figure.1 (c-i, ii, iii and iv)). The proposed IHC had an overall accuracy of 72%, a 'κ' of 0.66 and a JDMI of 0.56 (Table 1). The PR and RC of all urban feature categories obtained by the proposed IHC method were higher than for the benchmark methods (Table 1). Thus, the IHC layer was selected for the next step.

With respect to the classifiers, SegNet generated superior accuracy metrics in comparison with the benchmarks (Table 2). The accuracies of the urban landscape classes Bright_IS and Dark_IS increased significantly when SegNet was used (Table 2). Also, careful visual comparison between the ground reference map (Figure 1 (b-iv)), proposed IHC_SegNet (Figure 1(b-iii)) and the benchmark methods (Figure 1(d)) confirms that Unet, RF, SOM and RBF led to some pixel confusion. For example, the semi-natural class (Figure 1 (b-iii): yellow colour) was misclassified by the benchmark methods (Figure 2 (d)) while Dark_IS (Figure 1 (b-iii): red colour) was classified mistakenly as Non-IS (green colour) using such methods. Both Dark_IS and Semi_natural were identified correctly by the proposed SegNet (Figure 1 (b-iii)). It is noteworthy that the RF classifier yielded similar accuracy metrics to SegNet (Table 2). The high RF accuracy could be partly due to a false increase in PR and RC for some urban classes such as Dark_IS, water and shadow, and partly due to highly accurate detection of forested regions (Table 2).

5. Discussion

For the sake of succinctness, the discussion is restricted to the research questions in Section 1:

(1) Using KH-9 MCS, how can we effectively employ feature synthesis approaches to leverage urban spatial-contextual information for classification?

With respect to synthesizing features, our research demonstrated that a single panchromatic band of KH-9 MCS (SP_SegNet) was insufficient for RHFUL purposes (Table 1 and Figure 1(c-iv)). Our findings suggest that synthesizing new features such as those generated here can increase accuracy and facilitate historical urban mapping (Table 1, Figure 1(b and c)). Although benchmark methods showed some improvements above a single panchromatic band, they generated disappointing results due to a reliance on single types of features such as GLCM and Gabor textures. The proposed IHC approach employed internalized features, topological features, shape indicators, class variability and spatial hierarchy. This minimized the risk of loss of information. Despite this achievement, IHC features did not substantially increase the accuracy of the RHFUL map. Future research should, therefore, explore the application of other synthesizing feature approaches such as spatial–contextual information using adaptive techniques (Lv *et al.*, 2023b) and object-based morphological profiles (Geiss *et al.*, 2016).

(2) What type of labelling techniques are appropriate for KH-9 MCS over urban regions?

In terms of labelling, the proposed WSSL characterized accurately the semantic contents of urban landscapes in comparison with SAM models. Although SAM models are popular and powerful approaches for image labelling, we contend that the paucity of information on training SAM models (e.g., training images, architecture of the deep learning models) for analogue panchromatic imagery such as KH-9 MCS may lead to sub-optimal performance. Future research should explore re-training SAM models and other labelling techniques (e.g., Lv *et al.*, 2023a) for KH-9 MCS and other KH images (e.g., CORONA, ARGON).

(3) Which classification systems are the most efficient for reconstructing historical urban landscapes from KH-9 MCS images?

Focusing on classification, IHC_SegNet outperformed the benchmark classification systems by achieving the largest accuracy metrics and the best visual appearance. The promising performance of SegNet can be attributed to its architecture which considers appearance, shape and spatial relationships between different classes (Badrinarayanan *et al.*, 2017). Despite this promising performance, IHC_SegNet could not achieve an overall accuracy (OA) greater than 75%. This limitation might be due to the analogue structures of the KH-9 MCS image, while SegNet was designed for digital imagery (Please see supplementary: Figure 3). Future research will, therefore, search for appropriate deep learning architectures for KH-9 MCS images (Mboga *et al.*, 2020).

6. Conclusion

This research devised a systematic multi-stage RHFUL pipeline to tackle the challenges (single panchromatic band, labelling and classification) of reconstructing historical fine-scale urban landscape information from film based panchromatic KH-9 MCS imagery.

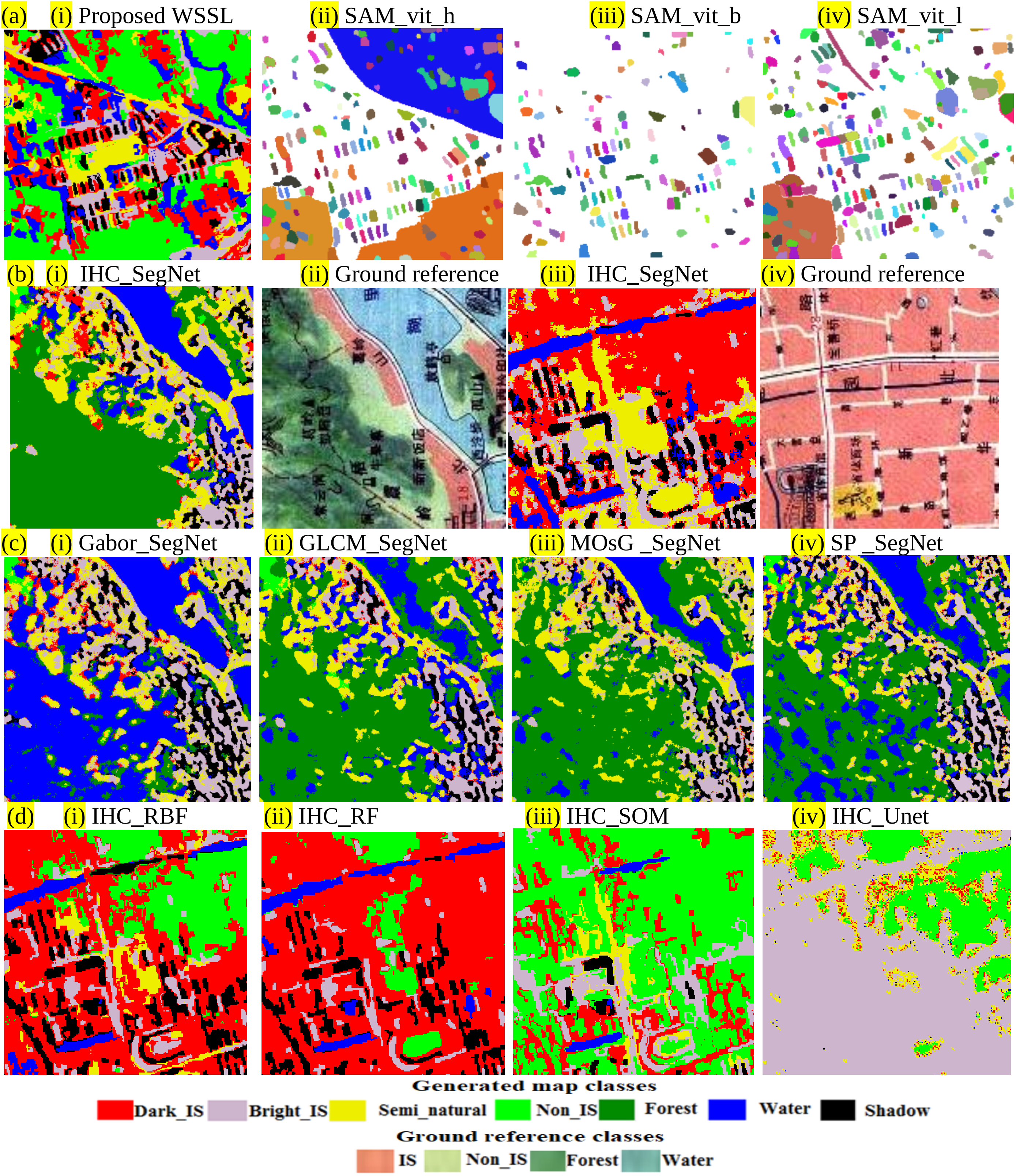

Figure. 1. (a) Comparison between the results of applying the proposed WSSL and other methods, (b) Comparison between the generated urban map via the proposed IHC_SegNet and ground reference map (Hangzhou Map 1983), (c) Generated urban maps by benchmark feature synthesizing methods and (d) Generated urban maps using benchmark classifiers.

Table 1, Comparison between accuracy of proposed IHC framework and benchmark approaches

Class	IHC_SegNet		Gabor_SegNet		GLCM_SegNet		MOsG_SegNet		SP_SegNet	
	RC	PR	RC	PR	RC	PR	RC	PR	RC	PR
Bright_IS	0.58	0.55	0.49	0.44	0.58	0.41	0.53	0.43	0.55	0.40
Dark_IS	0.43	0.56	0.25	0.46	0.15	0.36	0.18	0.36	0.13	0.32
Non_IS	0.70	0.85	0.58	0.79	0.53	0.71	0.63	0.74	0.60	0.72
Water	0.85	0.83	0.82	0.71	0.76	0.63	0.80	0.68	0.77	0.57
Shadow	0.76	0.56	0.66	0.42	0.65	0.41	0.64	0.43	0.64	0.35
Semi_natural	0.64	0.48	0.51	0.37	0.41	0.35	0.46	0.37	0.37	0.35
Forest	0.89	0.95	0.83	0.90	0.77	0.86	0.79	0.90	0.70	0.88
OA	0.72		0.62		0.58		0.61		0.56	
‘κ’	0.66		0.55		0.49		0.53		0.48	
JDMI	0.56		0.45		0.40		0.44		0.39	

Methods (column group heading above the method names)

Table 2, Comparison between accuracy of proposed deep learning SegNet and benchmark classifiers

Class	IHC_SegNet		IHC_RBF		IHC-RF		IHC_SOM		IHC_UNet	
	RC	PR	RC	PR	RC	PR	RC	PR	RC	PR
Bright_IS	0.58	0.55	0.45	0.62	0.36	0.77	0.41	0.57	0.88	0.27
Dark_IS	0.43	0.56	0.45	0.38	0.71	0.40	0.28	0.31	0.04	0.28
Non_IS	0.70	0.85	0.80	0.64	0.89	0.72	0.72	0.44	0.77	0.75
Water	0.85	0.83	0.77	0.87	0.78	0.97	0.64	0.71	0.69	0.93
Shadow	0.76	0.56	0.79	0.57	0.82	0.60	0.24	0.56	0.00	0.02
Semi_natural	0.64	0.48	0.44	0.57	0.36	0.56	0.32	0.52	0.14	0.25
Forest	0.89	0.95	0.89	0.87	0.94	0.92	0.83	0.78	0.91	0.94
OA	0.72		0.68		0.72		0.57		0.60	
‘κ’	0.66		0.62		0.67		0.48		0.52	
JDMI	0.56		0.52		0.56		0.40		0.43	

The proposed RHFUL was scrutinized and compared against state-of-the-art benchmark approaches. The main contributions of the proposed RHFUL pipeline are: (1) considering the scarcity of historical urban labels, the proposed WSSL accurately identified urban labels in the KH-9 MCS image, (2) the proposed IHC approach increased urban landscape mapping accuracy by a significant margin of 10% compared to the benchmarks, and (3) the IHC combined with the SegNet architecture produced the greatest classification accuracy compared to benchmark classifiers. Thus, the novel RHFUL pipeline proposed here should be of great interest to researchers and practitioners wishing to exploit the historical urban information latent in KH-9 MCS imagery. Moreover, further research in this direction on using KH-9 MCS imagery is needed, particularly based on recent advances in image classification, which may further address the challenges identified in this research.

Declaration of interests

No potential conflict of interest was reported by the authors.

Acknowledgements

We thank the Editors and anonymous reviewers for their very constructive comments.

Funding

This research was supported by Key Projects of Natural Science Research Projects in Colleges and Universities of Anhui Province (2022AH051126).

References

Badrinarayanan, V., A. Kendall, A., R. Cipolla, R., 2017. "SegNet: A Deep Convolutional Encoder-Decoder Architecture for Image Segmentation.". IEEE Transactions on Pattern Analysis and Machine Intelligence 39 2481-2495.

Benz, U.C., Hofmann, P., Willhauck, G., Lingenfelder, I., Heynen, M., 2004. Multi-resolution, object-oriented fuzzy analysis of remote sensing data for GIS-ready information. ISPRS Journal of Photogrammetry & Remote Sensing 58, 239-258.

Dehecq, A., Gardner, A.S., Alexandrov, O., McMichael, S., Hugonnet, R., Shean, D., Marty, M., 2020. Automated Processing of Declassified KH-9 Hexagon Satellite Images for Global Elevation Change Analysis Since the 1970s. Front. Earth Sci 8.

Fowler, M., 2016. The archaeological potential of declassified HEXAGON KH-9 panoramic camera satellite photographs. AARG News 53, 30-36.

Geiss, C., Klotz, M., Schmitt, A., Taubenbock, H., 2016. Object-Based Morphological Profiles for Classification of Remote Sensing Imagery. Ieee T Geosci Remote 54, 5952-5963.

Hammer, E., FitzPatrick, M., Ur, J., 2022. Succeeding CORONA: declassified HEXAGON intelligence imagery for archaeological and historical research. Antiquity 96 , Issue 387 , June 2022 , pp., 679 - 695.

Kirillov, A., Mintun, E., Ravi, N., Mao, H., Rolland, C., Gustafson, L., Xiao, T., Whitehead, S., Berg, A.C., Lo W.Y., Dollár, P., Girshick, R., 2023. Segment Anything. arXiv:2304.02643.

Lv, Z.Y., Huang, H., Sun, W., Jia, M., Benediktsson, J.A., Chen, F., 2023a. Iterative Training Sample Augmentation for Enhancing Land Cover Change Detection Performance With Deep Learning Neural Network. IEEE Transactions on Neural Networks and Learning Systems.

Lv, Z.Y., Zhong, P.D., Wang, W., You, Z.Z., Benediktsson, J.A., Shi, C., 2023b. Novel Piecewise Distance Based on Adaptive Region Key-Points Extraction for LCCD With VHR Remote-Sensing Images. Ieee T Geosci Remote 61.

Lv, Z.Y., Zhong, P.D., Wang, W., You, Z.Z., Falco, N., 2023c. Multiscale Attention Network Guided With Change Gradient Image for Land Cover Change Detection Using Remote Sensing Images. IEEE Geoscience and Remote Sensing Letters 20.

Marzolff, I., Kirchhoff, M., Stephan, R., Seeger, M., Aït Hssaine, A., Ries, J., 2022. Monitoring Dryland Trees With Remote Sensing. Part A: Beyond CORONA-Historical HEXAGON Satellite Imagery as a New Data Source for Mapping Open-Canopy Woodlands on the Tree Level. Front. Environ. Sci 10:896702.

Mboga, N., Grippa, T., Georganos, S., Vanhuysse, S., Smets, B., Dewitte, O., Wolf, E., Lennert, M., 2020. Fully convolutional networks for land cover classification from historical panchromatic aerial photographs. Isprs J Photogramm 167.

Pacifici, F., Chini, M., Emery, W.J., 2009. A neural network approach using multi-scale textural metrics from very high-resolution panchromatic imagery for urban land-use classification. Remote Sens Environ 113, 1276-1292.

Shahtahmassebi, A.R., Liu, M., Li, L., Wu, J., Zhao, M., Chen, X., Jiang, L., Huang, D., Hu, F., Huang, M., Deng, K., Huang, X., Shahtahmassebi, G., Biswas, A., Moore, N., Atkinson, P.M., 2023. De-noised and contrast enhanced KH-9 HEXAGON mapping and panoramic camera images for urban research,. Science of Remote Sensing 7.

Soille, P., 2003. Morphological image analysis : principles and applications. Springer, Berlin ; New York.